A Mutagenesis Study of the Putative Luciferin Binding Site Residues of Firefly Luciferase†

Bruce R. Branchini,*,‡ Tara L. Southworth,‡ Martha H. Murtiashaw,‡ Henrik Boije,§ and Sarah E. Fleet‡

Department of Chemistry, Connecticut College, New London, Connecticut 06320 USA, and Uppsala University, Uppsala, 75105 Sweden

Received April 21, 2003

ABSTRACT: Firefly luciferase catalyzes the highly efficient emission of yellow-green light from substrate firefly luciferin by a sequence of reactions that require Mg-ATP and molecular oxygen. We had previously developed [Branchini, B. R., Magyar, R. A., Murtiashaw, M. H., Anderson, S. M., and Zimmer, M. (1998) *Biochemistry 37*, 15311−15319] a molecular graphics-based working model of the luciferase active site starting with the first X-ray structure [Conti, E., Franks, N. P., and Brick, P. (1996) *Structure 4*, 287−298] of the enzyme without bound substrates. In our model, the luciferin binding site contains 15 residues that are within 5 Å of the substrate. Using site-directed mutagenesis, we made changes at all of these residues and report here the characterization of the corresponding expressed and purified proteins. Of the 15 residues studied, 12 had a significantly (≥4-fold K_m difference) altered binding affinity for luciferin and seven residues, spanning the primary sequence region Arg218−Ala348, had substantially (≥30 nm) red-shifted bioluminescence emission maxima when mutated. We report here an interpretation of the roles of the mutated residues in substrate binding and bioluminescence color determination. The results of this study generally substantiate the accuracy of our model and provide the foundation for future experiments designed to alter the substrate specificity of firefly luciferase.

The firefly's flashing lights beautifully illustrate bioluminescence, the conversion of chemical energy into light by a living organism. Research mainly focused on the North American firefly *Photinus pyralis* (*1*−*4*) has progressed toward a very good understanding of the chemical transformations leading to light emission. A wide variety of applications of firefly bioluminescence include in vivo luminescence monitoring (*5*, *6*) as well as medical and pharmaceutical methods, many of which use the firefly luciferase gene as a reporter of gene expression and regulation (*7*−*9*).

As indicated in Figure 1, the luciferase enzyme (Luc)[1] functions as a monooxygenase, although it does so without the apparent involvement of a metal or cofactor. The multistep oxidation of the luciferyl-adenylate (D-LH_2-AMP) results in the production of electronically excited oxyluciferin and CO_2, both containing one oxygen atom from molecular oxygen. It is probable that the excited state product is formed from a dioxetanone intermediate through an intramolecular chemically initiated electron-exchange luminescence mechanism (*10*). Relaxation of excited-state oxyluciferin to the corresponding ground state is accompanied by the emission of light. A quantum yield of ∼0.9 for this process (*11*) requires an efficient catalytic machinery and a highly favorable environment for the radiative decay of an excited state.

The cloning and sequencing of *P. pyralis* luciferase and similar enzymes from 14 other beetle species[2] (*12*−*17*) have revealed that these luciferases are closely related to a large family of nonbioluminescent proteins (*18*, *19*) that catalyze reactions of ATP with carboxylate substrates to form acyl-adenylates. The luciferase-catalyzed formation of enzyme-bound D-LH_2-AMP (Figure 1, step a) is an example of this common chemistry. The "acyl-adenylate/thioester-forming" superfamily of enzymes (*20*) includes a variety of acyl:CoA ligases; the acyl-adenylate-forming domains of enzyme complexes involved in the nonribosomal synthesis of peptides and polyketides; the luciferases; and several other types of enzymes. In the second half-reaction, most of these enzymes generate thioester (e.g., of CoA) intermediates or products from the initially formed corresponding acyl-adenylates;

† This work was supported by a grant from the National Science Foundation (MCB 0130908), the Hans & Ella McCollum '21 Vahlteich Endowment and the Nancy Batson Nisbet Rash Faculty Research Award for 2002.

* To whom correspondence should be addressed: Department of Chemistry, Connecticut College, 270 Mohegan Avenue, New London, CT 06320. Tel.: (860) 439-2479. Fax: (860) 439-2477. E-mail: brbra@conncoll.edu.

‡ Connecticut College.

§ Uppsala University.

[1] Abbreviations: Acs, acetyl-CoA synthetase from *Salmonella enterica*; CB, 50 mM Tris-HCl (pH 7.0), 150 mM NaCl, 1 mM EDTA and 1 mM DTT; DHB, 2′-3′-dihydroxybenzoate; DhbE, the 2′-3′-dihydroxybenzoate adenylation domain for bacillibactin synthesis in *Bacillus subtilis*; GST, glutathione-*S*-transferase; Luc, *Photinus pyralis* luciferase (E.C. 1.13.12.7); D-LH_2, D-firefly luciferin; D-LH_2-AMP, luciferyl-*O*-adenosine monophosphate; PheA, the phenylalanine-activating subunit of gramicidin synthetase 1; NRPS, nonribosomal peptide synthetase; PplGR, recombinant *Pyrophorus plagiophthalamus* green emitting luciferase isozyme containing the additional N-terminal peptide GPLGS-; WT, recombinant *Photinus pyralis* luciferase containing the additional N-terminal peptide GPLGS-.

[2] The deduced amino acid sequence of *Phengodes species* luciferase was provided by K. V. Wood and M. Gruber, personal communication.

10.1021/bi030099x CCC: $25.00
Published on Web 08/13/2003

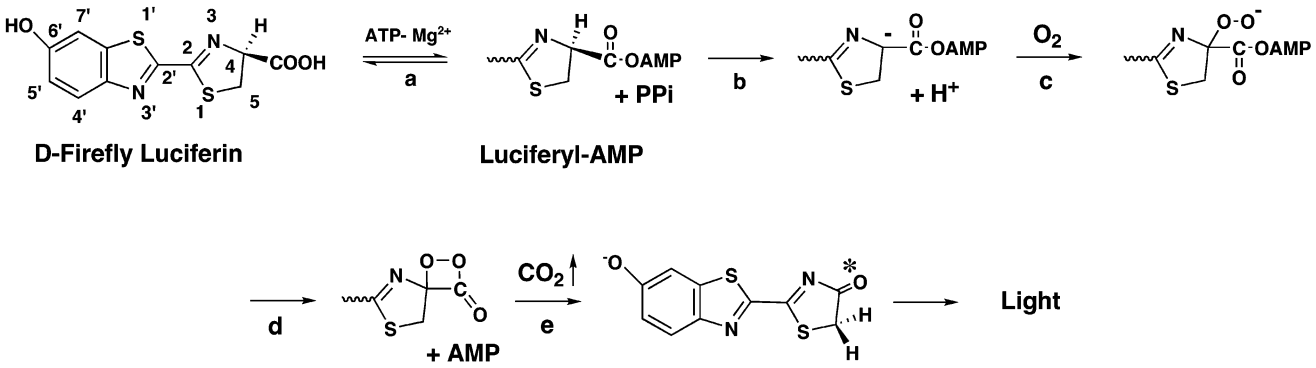

FIGURE 1: Mechanism of firefly luciferase-catalyzed bioluminescence.

these reactions are similar to one suggested (*21*) to account for the stimulatory effect of CoA on luciferase activity. The second function of luciferase is to oxidize D-LH_2-AMP (Figure 1, steps b−e); however, Luc also functions as a ligase in the production of diadenosine tetraphosphate (*22*).

There are presently X-ray structures of four members of the "acyl-adenylate/thioester-forming" superfamily (*20*). The Luc crystal structure without bound substrates (*23*), the landmark structure, revealed a unique molecular architecture consisting of a large N-terminal domain (residues 1−436) and a small C-terminal domain (residues 440−550), separated by a short linker peptide. Additionally, a crystal structure of Luc containing two molecules of bromoform, a general anesthetic, and a largely reversible Luc inhibitor with respect to D-LH_2, was obtained (*24*). One bromoform molecule was found to bind at a site proposed to be the tentative D-LH_2 binding pocket in Luc and only local conformational changes mainly in the Ser314−Leu319 loop of the N-domain accompanied anesthetic binding (*24*).

Next, the crystal structure of the phenylalanine-activating subunit of gramicidin synthetase 1 (PheA) in a complex with Phe, Mg ion, and AMP was reported (*25*). The active site of PheA was determined to be at the interface of the two domains, which were remarkably similar in size and shape to the corresponding domains of Luc despite the low (16%) sequence identity. In the PheA structure, however, the C-terminal domain was rotated 94° and was 5 Å closer to the N-terminal domain than in the "open" (*24*) Luc structure. The crystal structure of DhbE, the 2′-3′-dihydroxybenzoate adenylation domain for bacillibactin synthesis in *Bacillus subtilis*, was determined (*26*) more recently. Together with two other gene products produced by the *dhb* operon, DhbE, like PheA, forms a nonribosomal peptide synthetase (NRPS). The structure was revealed in the enzyme's native state, with bound adenylate (DHB-AMP), and like PheA, with its hydrolyzed adenylate products AMP and carboxylate substrate (DHB). The DhbE crystal structure in all three states displays the same relative orientation of the C-domain as PheA, rotated compared to the Luc structure, suggesting that only local conformational changes occur with substrate binding (*26*).

Very recently, the crystal structure of acetyl-CoA synthetase (Acs) complexed with adenosine-5′-propyl phosphate, a nonreactive acyl-adenylate analogue, and CoA was reported (*27*). While the overall fold and secondary structural elements are similar to those seen in the three previously reported structures, the C-terminal domain is rotated ∼140° relative to the conformation of PheA and DhbE. Gulick and coworkers have proposed (*27*) that the formation of the acyl-adenylate from the natural substrates would occur in a conformation of Acs such as that found in PheA and DhbE. The newly identified conformation of Acs would then be formed by rotation of the C-terminal domain as a result of CoA binding. This third conformation for adenylate-forming enzymes would develop the entire active site for the second half-reaction, the displacement of AMP by CoA to form the corresponding acyl-CoA. Assuming that the conformation of Luc in the crystal structure is physiologically relevant, the formation and oxidation of D-LH_2-AMP would require rotation of the C-terminal domain into one or more conformations, possibly similar to those revealed by the structures of PheA, DhbE, and Acs.

Starting with the structures of Luc (*23*) and PheA (*25*), we used molecular modeling techniques to produce a potential working model of the Luc active site containing substrates D-LH_2 and Mg-ATP (*28*). Our working model has been quite useful in the rational design of site-directed mutagenesis-based Luc structure−function studies, including several related to the determination of bioluminescence color (*29*−*31*). In the study reported here, we used a site-directed mutagenesis approach to examine the role of amino acid residues that our working model predicts to be within 5 Å of bound D-LH_2. The putative D-LH_2 binding site we have proposed is generally quite similar to the sites identified from the bromoform-containing Luc structure (*24*) and the Luc-ATP−luciferin complex produced by another molecular model (*32*). One point of difference, strongly supported by subsequent mutagenesis results (*31*), is that our model shows that Arg218, and not Arg337, is at the base of the D-LH_2 binding pocket (Figure 2). In our model, 15 amino acid residues are included in the proposed D-LH_2 binding site. In an effort to determine substrate specificity-conferring Luc residues and to further evaluate our model, a site-directed mutagenesis-based approach was undertaken to investigate the role of the 15 luciferase amino acid residues.

MATERIALS AND METHODS

Materials. The following items were obtained from the indicated sources: Mg-ATP (bacterial) (Sigma); D-LH_2 (Biosynth AG); restriction endonucleases, T4 polynucleotide kinase and T4 DNA ligase (New England Biolabs); and mutagenic oligonucleotides (Invitrogen). Ppy WT, R218A, H245A, T343A, and K529A luciferases were constructed and purified as previously reported (*28*−*31*).

General Methods. Detailed procedures including descriptions of the equipment used to determine bioluminescence

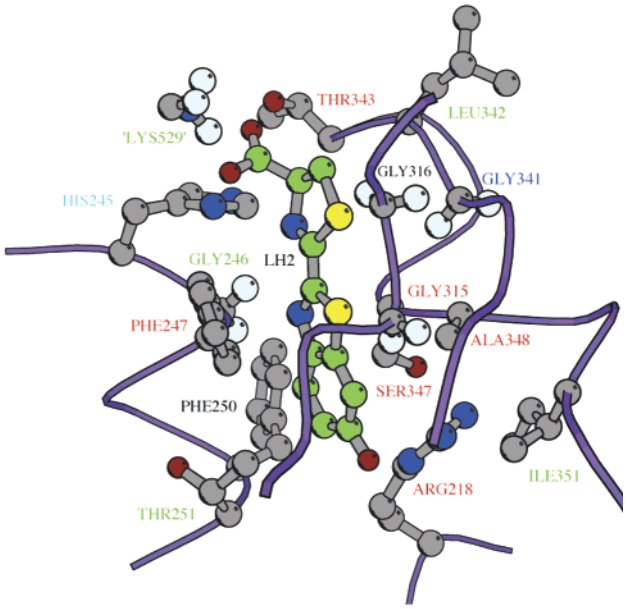

FIGURE 2: Diagram showing the residues within 5 Å of D-LH_2 at the putative luciferase substrate binding site suggested (*28*) by molecular modeling of Luc with D-LH_2 and ATP (not shown) and Mg^{2+} ion (not shown). The model was created starting with the Luc X-ray structure 1LCI (*23*), and methylammonium ion (labeled Lys529) was used to represent possible interactions of the Lys529 side-chain. Traces through the α-carbons of regions Val217−Phe219, His244−Thr252, Ile312−Pro318, and Arg337−Pro353 are shown as purple coils. This diagram was generated using the program MOLSCRIPT (*46*). The residue labels are color coded to indicate the major effects (≥4-fold K_m difference, ≥30 nm red-shifted emission or <5% of total WT bioluminescence) of the mutations: red, D-LH_2 binding and bioluminescence color; cyan, bioluminescence color; green, D-LH_2 binding; blue, D-LH_2 binding and specific activity; and black, none. With the exception of G341A, S347A, and I351A, all the enzymes with substantially altered K_m values for D-LH_2 also had significantly altered K_m values for Mg-ATP.

activity of the luciferases by flash height- and integration-based light assays have been described previously (*28*−*31*, *33*, *34*). Flash height-based specific activity measurements using HPLC-purified synthetic D-LH_2-AMP (*35*, *36*) were performed as previously described (*30*) in 50 mM glycylglycine buffer, pH 7.8, containing 0.1 mL aliquots of D-LH_2-AMP stock solution in 10 mM sodium acetate, pH 4.5. Assays (0.51 mL) contained saturating concentrations of D-LH_2-AMP and were initiated by the injection of 1−3 μg of luciferase.

Mass spectral analyses of the proteins were performed by tandem HPLC-electrospray ionization mass spectrometry using a PerkinElmer Series 200 HPLC system and a Sciex ABI150A mass spectrometer. The new luciferases reported here had calculated molecular masses (Da) of G246A, 61 171; F247A, 61 081; F247L, 61 123; F247Y, 61 173; F250G, 61 067; F250S, 61 097; T251A, 61 127; G315A, 61 171; G316A, 61 171; G341A, 61 171; L342A, 61 115; S347A, 61 141; A348V, 61 185; and I351A, 61 115. The actual mass values were all within the allowable experimental error of 0.01% of the calculated values. The mutations of all luciferase genes were verified by DNA sequencing performed at the W. M. Keck Biotechnology Laboratory at Yale University.

Site-Directed Mutagenesis. The mutants F247A and S347A were created by oligonucleotide-directed mutagenesis (*37*), as previously described (*28*). The following mutagenic primers were designed for annealing onto the ssDNA template: F247A, 5′-T TTA AGT GTG GTA CCA TTC CAT CAC GGT **GCT** GGA ATG TT T-3′ [*Kpn*I] and S347A, 5′-GAG ACT ACT **GCA** GCT ATT CTG ATT ACA CCC-3′ [*Pst*I] (underline represents silent changes to create a unique screening endonuclease site, the bold represents the mutated codon, and brackets indicate the screening endonuclease). To produce the mutant luciferases G246A, F247L, F247Y, and F250G, mutagenesis of WT in the pGex-6P-2 vector was performed with the Chameleon double-stranded mutagenesis kit (Stratagene) using *Alwn*I as the selection endonuclease. Site-directed mutagenesis was carried out according to the manufacturer's instructions using the primers: G246A, 5′-CCA TTC CAT CAC **GCG** TTT GGA ATG TTT AC-3′ [*Mlu*I]; F247L, 5′-GTT CCA TTC CAC CAT GGT **TTG** GGA ATG TTT AC-3′ [*Nco*I]; F247Y, 5′-GTT CCA TTC CAC CAT GGT **TAT** GGA ATG TTT AC-3′ [*Nco*I]; F250G, 5′-C GGT TTT GGA ATG **GGT** ACC ACA CTC GGA-3′ [*Kpn*I]. The primer 5′-TCC TGT TAC CAG TCG CGA CTG CCA GTG-3′ [*Nru*I] was included in all reactions to eliminate an *Alwn*I selection site.

The QuikChange Site-Directed Mutagenesis kit (Stratagene) was used to create the remaining mutant luciferase proteins. Site-directed mutagenesis was carried out according to the manufacturer's instructions using WT in the pGex-6P-2 vector as a template and the following primers and their respective reverse complements: F250S, 5′-CCA TTC CAT CAC GGT TTT GGA ATG **TCG** ACT ACA CTC GG-3′ [*Sal*I]; T251A, 5′-GGT TTT GGA ATG TTT **GCT** ACA CTC GGA TAT CTG ATA TGT GG-3′ [*Eco*RV]; G315A, 5′-CAC GAA ATT GCT TCT GCG GGC **GCC** CCT CTT TCG AAA-3′ [*Kas*I]; G316A, 5′-AA ATT GCT TCT GGC **GCC** GCA CCT CTT TCG-3′ [*Kas*I]; G341A, 5′-CTT CCA GGG ATA CGC CAA GGA TAT **GCG** CTC ACT GAG ACT-3′ [*Sty*I]; L342A, 5′-CCA GGG ATA CGC CAA GGA TAT GGG **GCC** ACT GAG ACT-3′ [*Sty*I]; A348V, 5′-GGG CTC ACT GAG ACT ACT AGT **GTT** ATT CTG ATT ACA CCC GAG-3′ [*Spe*I]; I351A, 5′-GGG CTC ACT GAG ACT ACT AGT GCT ATT CTG **GCT** ACA CCC GAG GGG-3′ [*Spe*I].

Steady-State Kinetic Constants. Values of K_m and V_{max} for D-LH_2 and Mg-ATP for all luciferases were determined from bioluminescence activity assays in which measurements of maximal light intensities were taken as estimates of initial velocities. Data were collected for reactions in 25 mM glycylglycine buffer, pH 7.8, and were analyzed as described earlier (*28*).

Bioluminescence Emission Spectra. Bioluminescence emission spectra for the luciferases with D-LH_2 and Mg-ATP were obtained using a PerkinElmer LS55 luminescence spectrometer operated in the "bioluminescence" mode, under conditions that have been described in detail elsewhere (*33*). Data were collected over the wavelength range 480−680 nm in a 1 mL optical glass cuvette. Gate and delay times, detector voltage, scan rate, and slit width were adjusted to optimize instrument response. Data were corrected for the spectral response of the R928 photomultiplier tube using the PerkinElmer FL WinLab software. Bioluminescence emission spectra were obtained with 2 mM Mg-ATP and 70 μM D-LH_2 in 25 mM glycylglycine buffer, pH 7.8, with final concentrations of luciferases ranging from 0.1 to 3.0 μM. The

Enzyme	Comparison of Carboxylate Substrate and Putative D-LH$_2$ Binding Site Residues														
Luc	R218	H245	G246	F247	F250	T251	G315	G316	G341	L342	T343	S347	A348	I351	K529
PheA	L210	F234	**D235**	**A236**	**W239**	E240	**A301**	G302	G324	P325	T326	**I330**	**C331**	T334	**K517**
DhbE	S210	H234	**N235**	**Y236**	**S239**	S240	**G306**	G307	G331	M332	A333	**V337**	**N338**	R341	**K519**
Acs	A285	W309	V310	T311	Y315	L316	V386	G387	W414	Q415	T416	G420	F421	T424	K609

FIGURE 3: Deduced amino acid sequence comparison of residues within 5 Å of D-LH$_2$ in the Luc molecular model (*28*) to corresponding residues of PheA (*25*), DhbE (*26*), and Acs (*27*). Underlined amino acids are absolutely conserved among the luciferases. PheA and DhbE residues in bold confer carboxylate substrate specificity in the NRPSs (*44*, *45*) and DhbE (*26*). The Luc residue labels are color coded to indicate the major effects (≥4-fold K_m difference, ≥30 nm red-shifted emission or <5% of total WT bioluminescence) of the mutations: red, D-LH$_2$ binding and bioluminescence color; cyan, bioluminescence color; green, D-LH$_2$ binding; blue, D-LH$_2$ binding and specific activity; and black, none. With the exception of G341A, S347A, and I351A, all the enzymes with substantially altered K_m values for D-LH$_2$ also had significantly altered K_m values for Mg-ATP.

Table 1: Steady State Kinetic Constants and Bioluminescence Emission for Luciferase Enzymes at pH 7.8

	D-LH$_2$		Mg-ATP	
enzyme	K_m (μM)[a]	k_{cat} (s^{-1})[b]	K_m (μM)	bioluminescence maximum[c] (nm)
WT	15.0	0.125	160.0	557 (66)
R218A	301.0	0.004	6200.0	611 (84)
H245A	15.0	0.041	240.0	604 (93)
G246A	4.2	0.060	29.0	556 (66)
F247A	230.0	0.007	3500.0	587 (95)
F247L	124.0	0.116	226.0	565 (74)
F247Y	18.0	0.098	80.0	557 (66)
F250G	15.7	0.013	166.0	558 (67)
F250S	22.0	0.036	133.0	557 (97)
T251A	311.0	0.043	2000.0	556 (72)
G315A	200.0	0.0002	1200.0	607 (53)
G316A	18.0	0.049	107.0	578 (84)
G341A	60.0	0.0002	200.0	557 (73)
L342A	130.0	0.106	1200.0	554 (63)
T343A	99.0	0.001	857.0	617 (65)
S347A	170.0	0.030	344.0	557:601 (105)[d]
A348V	133.0	0.064	1038.0	610 (78)
I351A	85.0	0.190	285.0	573 (73)
K529A	230.0	0.0001	1200.0	562 (93)

[a] Kinetic constants were determined as previously described (*29*−*31*, *33*). The error associated with K_m values falls within ±10% of the value. [b] V_{max} values determined with each enzyme were expressed in units of einstein × 10^{-6} s^{-1}. The corresponding k_{cat} values were obtained from the data used to determine the K_m values for D-LH$_2$ by dividing the V_{max} values by the final amount (μmol) of each enzyme in the assay mixtures. The error associated with these measurements falls within ±15% of the value. [c] Bioluminescence emission spectra were measured at pH 7.8 as described in Materials and Methods. Bandwidths (nm) at 50% of emission maxima are indicated in parentheses. [d] In this mutant, two clear maxima were observed and the ratio of the intensities was 2:1 for the 601 and 557 nm emissions, respectively.

stabilizing storage reagents NaCl, ammonium sulfate and glycerol were kept at standard concentrations of 7.2 mM, 38 mM, and 0.1%, respectively.

RESULTS AND DISCUSSION

Rationale for Mutagenesis. An alanine-scanning mutagenesis approach was taken to study 15 putative D-LH$_2$ binding site residues (Figure 3). Additionally, the Luc enzymes F250G and F250S were available from an ongoing study in our laboratory (unpublished results). Since the position 250 mutants had normal K_m values for D-LH$_2$ and Mg-ATP (Table 1), we did not prepare the F250A luciferase. Ala348 was changed to Val to evaluate the effects of introducing a larger and branched nonpolar side-chain. Phe247 was mutated to Leu and Tyr in addition to Ala, to specifically evaluate our previous proposal (*28*) that this invariant residue among the luciferases may participate in D-LH$_2$ binding through a π-stacking interaction.

Overexpression, Purification, and Characterization of the Luciferase Proteins. WT and the modified luciferases were expressed as GST-fusion proteins and contained the additional N-terminal peptide GPLGS- (*28*, *29*), which remained after PreScission protease cleavage from GST. Average yields (mg) of purified proteins per 0.5 L cultures were WT (8.0), R218A (2.4), H245A (4.6), G246A (5.0), F247A (8.9), F247L (5.0), F247Y (9.4), F250S (12.0), F250G (1.2), T251A (4.0), G315A (8.0), G316A (4.0), G341A (8.5), L342A (4.1), T343A (2.6), S347A (4.8), A348V (0.4), I351A (8.0), K529A (4.7). All enzymes maintained full activity for at least 3 months when stored at 4 °C in CB containing 0.8 M ammonium sulfate and 2% glycerol.

Effects of Luciferase Mutations on Substrate Binding, Catalytic Constants, and Bioluminescence Activity. To evaluate the effects of amino acid substitutions on the kinetic behavior of the enzymes containing changes in the 15 targeted residues, the steady-state kinetic parameters for the WT and modified luciferases were determined (Tables 1 and 2). Specific activities (Table 2) for the enzymes were measured with saturating concentrations of the natural substrates, corrected for the response of the detector to differences in their emission spectra (*24*) and were expressed relative to WT. The flash height-based values relate the maximum achievable overall reaction rates for the combined adenylation and oxidation steps (Figure 1, steps a−e); however, they are independent of the time required to reach maximum light output (rise time). Typically, rise times were ∼0.5 s and varied from 0.3 to 2.0 s. Integration-based specific activities reflect total bioluminescence output and differences between flash height-based values are mainly determined by the rates of light emission decay. With the exception of G316A, the integration-based specific activities of all of the mutant Luc enzymes were greater than the corresponding flash height-based ones. While six of the mutants had flash height-based specific activities less than 5% of WT, only G341A produced less than 5% of the total bioluminescence of WT (Table 2).

Measurements of the kinetic properties of WT and the Luc mutants with synthetic D-LH$_2$-AMP were undertaken to evaluate the effects of the amino acid changes specifically on the luciferase-catalyzed oxidative chemistry (Figure 1, steps b−e), after and independent of adenylate formation (Figure 1, step a). The light emission profiles (rise and decay times) of all the luciferase mutants with the preformed adenylate were similar to WT (data not shown). Five of the

Table 2: Bioluminescence Activity of Luciferase Enzymes at pH 7.8

enzyme	relative specific activity with D-LH_2 and Mg-ATP[a] flash height	integrated	rise time[b] (s ± 0.15)	decay time[c] (min ± 0.01)	relative specific activity with D-LH_2-AMP[d] flash height
WT	100.0	100.0	0.5	0.2	100.0
R218A	3.6	30.0	1.2	4.4	9.6
H245A	26.4	80.0	0.9	0.9	72.0
G246A	44.0	104.0	0.8	0.2	48.0
F247A	4.0	57.0	0.9	7.8	5.4
F247L	89.0	307.0	0.6	1.3	140.0
F247Y	71.0	84.0	0.4	0.2	63.0
F250G	7.5	23.0	2.0	3.4	31.0
F250S	21.7	25.0	0.5	0.2	45.0
T251A	29.0	156.0	0.6	2.9	20.0
G315A	0.15	20.4	1.4	62.3	11.2
G316A	31.7	5.7	0.3	0.1	36.0
G341A	0.16	3.0	1.1	14.3	0.9
L342A	56.0	730.0	0.8	9.4	59.0
T343A	1.1	19.5	1.8	8.9	11.0
S347A	16.7	97.2	0.6	2.4	72.0
A348V	41.0	150.0	0.6	4.6	132.0
I351A	139.0	547.0	0.5	0.5	109.0
K529A	0.06	12.5	0.6	106.0	50.0

[a] Specific activity measurements (flash height- and integration-based) were made at pH 7.8 with D-LH_2 and Mg-ATP as previously described (*28*−*30*, *33*) using saturating concentrations of substrates. Specific activity data are expressed relative to WT values which are defined as 100 and are equivalent to 1.18×10^{15} photons s^{-1} mg^{-1} (0.12 einstein $\times$ 10^{-6} s^{-1} μmol^{-1}) and 2.45×10^{16} photons mg^{-1} (2.5 einstein $\times$ 10^{-6} μmol^{-1}) for flash height-based and integration-based assays, respectively. Light intensity data were corrected for the spectral response of the Hamamatsu 931B photomultiplier tube and differences in the bandwidths of the emission spectra (*28*, *29*). [b] Rise time measurements represent the time interval until maximum flash height is attained following the injection of Mg-ATP to initiate the reaction. The estimated mixing time is 0.2 s and data are acquired at a sampling rate of 0.05 s (*29*−*31*). [c] Decay time measurements represent the time interval from attainment of maximum flash height to 20% of the maximum emission intensity. [d] Flash height specific activity measurements were made using saturating concentrations of synthetic D-LH_2-AMP as described in Materials and Methods. The error associated with specific activity measurements is ±10% of the value.

mutants, R218A, F247A, G315A, G341A, and T343A showed at least a ∼10-fold reduced capability to produce light from D-LH_2-AMP compared to WT (Table 2). The G341A enzyme, the poorest of these mutants, was also seriously compromised in its ability to produce the adenylate.

Mutations Affecting D-LH_2 and Mg-ATP Substrate Binding. The luciferase mutants R218A, G246A, F247A, T251A, G315A, L342A, T343A, A348V, and K529A had significantly altered binding affinities for both natural substrates (Table 1). Previously, we proposed (*28*, *29*) that the catalytic function of Thr343 was to orient the carboxylate of D-LH_2 for reaction at the α-phosphate of ATP and possibly also to stabilize the resulting pentavalent transition state leading to efficient adenylate production. Gly315, absolutely conserved among the luciferases and located in a mobile loop (residues Ser314−Leu319), provides conformational flexibility that is apparently essential for overall enzyme activity as well as substrate binding.

Our full model of the Luc active site (*28*) includes the ATP and D-LH_2 binding sites in close proximity with Lys529 making electrostatic interactions to D-LH_2 and ATP. Arg218 is at the bottom of an active site containing shared binding site regions Gly315−Pro318 and Gly339−Thr343. The latter residues, found in a β-hairpin motif made up of strands B7 and B8 (*23*), are part of the highly conserved structural motif II (*20*) (^{340}YGLTE^{344} in Luc) of the acyl-adenylate-forming enzyme family. In our model (Figure 2), the Arg218 side-chain is hydrogen-bonded to the hydroxyl group of Ser347 and the main chain carbonyl group of Ala348, thereby bringing helix 7 (*23*) into proximity with the β-hairpin motif.

With the exception of the results for residues Gly246, Phe247, and Thr251, the mutations affecting both K_m values were in residues proximal to both binding sites. Residues 246, 247, and 251 are found in helix 8 (*23*), part of a β−α−β motif comprised of residues Ala236−Leu264. Residues Gly246−Thr251 of helix 8 form one side of the D-LH_2 binding pocket, which includes the peptide ^{244}HHGF^{247}, the target of highly specific photooxidation by a D-LH_2 analogue (*38*). Alanine mutations at Gly246, Phe247, and Thr251 may alter the stability of the helix within a motif that is apparently important for the structural integrity of both substrate binding sites. The K_m values of the G246A enzyme for D-LH_2 and Mg-ATP (4.2 and 29 μM, respectively) were ∼4−5-fold less than WT (Table 1). Thus, the methyl side-chain of Ala is evidently well accommodated, even though in our model (Figure 2), an α-H of Gly246 is located within ∼3 Å of the D-LH_2 thiazoline ring. Interestingly, the K_m values of the *Pyrophorus plagiophthalamus* green emitting luciferase isozyme (PplGR), which has Ala at position 243 (Gly246 in Luc), were also approximately ∼4-fold lower than WT (unpublished results). The Ala243 to Gly mutation introduced into PplGR resulted in K_m values approximately equivalent to WT (unpublished results). Evidently, the position 246/243 side-chain is a strong determinant of the differences in the binding properties of the two luciferases. Additional examples of A243G mutations in railroad worm and click beetle luciferases causing changes in K_m values for D-LH_2 have been reported (*39*). Moreover, the importance of the β−α−β motif is substantiated by previously reported (*28*) K_m values for a H244F mutant that are nearly identical to those obtained with G246A.

The mutation of Phe247 to Ala results in 15- and 22-fold increases in K_m values for D-LH_2 and Mg-ATP, respectively. While the removal of the phenyl group elevated the K_m values of both substrates, this was not the case for the F247L and F247Y enzymes (Table 1). The F247L protein had a normal affinity for Mg-ATP, while the 8-fold higher K_m for D-LH_2 suggests that replacing the phenyl side-chain with another large hydrophobic group is not sufficient to restore normal D-LH_2 binding. Replacing Phe247 with the aromatic phenol side-chain of Tyr, however, nearly restored the K_m value for D-LH_2 to the wild-type value, while reducing the K_m for Mg-ATP 2-fold. It appears that the long-range effects of the Phe247 side-chain replacements on Mg-ATP binding are different from the local effects at the D-LH_2 site. Effective D-LH_2 binding requires the aromatic phenyl ring at position 247 and aromaticity is the key determinant. The mutational studies of Phe247 provide experimental support for our previous proposal (*28*) that this invariant residue among the luciferases participates in D-LH_2 binding through a π-stacking interaction with the benzothiazole ring.

Mutations Affecting Only D-LH_2 Binding. The luciferase mutants F247L (discussed above), S347A, and I351A

displayed significantly diminished affinity for D-LH_2, yet had near normal K_m values for Mg-ATP (Table 1). The fairly specific effects of the alanine substitutions solidify the inclusion of these residues in the positions shown in our model of the D-LH_2 binding site. The side-chain hydroxyl of Ser347 is located near the benzothiazole ring of D-LH_2 (Figure 2). The nonpolar side-chain of Ile351 is also near the benzothiazole ring and far removed from the ATP binding site, a position consistent with the specific effect of the Ala substitution. The G341A mutant had a nearly normal K_m for Mg-ATP and a 4-fold elevated K_m for D-LH_2. The 625-fold decreased k_{cat} value of the G341A mutant for the overall bioluminescence process as well as the very poor catalytic ability of this enzyme to produce light from synthetic D-LH_2-AMP strongly suggest that this Gly residue has a key role in catalysis. Appending a methyl side-chain evidently creates structural changes that disrupt the normal functioning of motif II (*20*) in which Gly 341 is located. A further investigation of the role Gly341 in luciferase catalysis is ongoing.

Mutations Having No Effect on Substrate Binding or Catalysis. Changing residues His245 and Gly316 to Ala, as well as replacing Phe250 with Gly and Ser, produced enzymes with almost normal catalytic and substrate binding properties (Tables 1 and 2). The role of His245 had been examined previously by extensive mutagenesis (*28*, *29*) and site-directed photooxidation studies (*38*). His245 is absolutely conserved in all luciferases, and our model shows the side-chain imidazole at the opening of the luciferin binding pocket in close proximity to the D-LH_2 carboxylate. The ability of Luc to accommodate Ala well at position 316 is understandable since this residue is found at the equivalent position in five click beetle sequences. Moreover, Gly316, unlike adjacent mobile loop residue Gly315, has dihedral angles that could be reasonably accommodated by an Ala residue (*40*). In our model, the side-chain phenyl ring of Phe250 is shown within ~3 Å of the D-LH_2 benzothiazole ring, but unlike Phe247, it does not make a π-stacking interaction with the substrate. Ser and Gly are found at positions equivalent to Phe250 in the five click beetle sequences that also have Ala in place of Gly316.

Mutations Affecting Bioluminescence Color. Among the group of 15 putative D-LH_2 contact residues, mutations at nine positions produced bioluminescence emission maxima that were red-shifted by at least 15 nm (Table 1). There were shifts of 15−21 nm in the G316A and I351A enzymes, a more extensive 30 nm change in the F247A protein, and substantial increases (44−60 nm) in the emission maxima of the R218A, H245A, G315A, T343A, S347A, and A348V luciferases. No absolute and straightforward correlations can be made between any of the shared characteristics of these residues (e.g., location in structural elements, conservation among luciferase primary sequences, or kinetic parameters) and their ability to alter bioluminescence color. In general, however, support for our model was provided by our findings that bioluminescence color is altered by many of the changes at residues of the putative substrate/emitter binding site.

The major finding from the mutation of four helix 8 residues is that a phenyl ring at position 247 is necessary for normal emission color. The role of the N-cap residue His245 in maintaining normal bioluminescence color in Luc has been presented previously (*28*, *29*). The finding that both the F250S and F250G mutants catalyzed normal yellow-green light emission was especially surprising. For the click beetle isozymes, the Ser247 (Phe250 in Luc) to Gly change is largely responsible for changing the color of emitted light from yellow to orange (*2*, *12*). Viviani et al. (*39*) have conducted mutagenesis studies at position 246/243 in several other firefly and click beetle species. They concluded that this position influences bioluminescence color in pH-insensitive luciferases as well as the property of pH sensitivity itself in true fireflies. Our data, however, do not support the latter point because the Luc G246A and Phe250 mutants had unchanged emission color and retained pH sensitivity (data not shown).

The Ala mutations at Gly315 and Gly316 of the Ser314−Leu319 mobile loop both produced red-shifted emission spectra. Taken together with the kinetic results discussed above, conformational changes in this loop may not only be necessary for substrate binding (*24*), but also may preserve the local environment around the light emitting oxyluciferin.

Within the β-hairpin motif (residues Gly339−Ile351), changes at positions 341 and 342 had no effect on the color of bioluminescence; however, the five mutations at residues in the region Thr343−Ile351 produced red-shifted emission profiles. We had previously proposed (*29*) roles for Thr343 in alternative speculative mechanisms of emission color. In view of our finding (*33*) that the enol form of oxyluciferin is not required to explain green bioluminescence, we believe that the invariant Thr343 provides key hydrogen-bonding interactions that directly or indirectly maintain the keto form of the emitter in the proper position for normal bioluminescence. The Ile to Ala change at position 351 produced an enzyme whose bioluminescence was shifted to 573 nm. Moreover, this color change was accompanied only by an increase (~5-fold) in K_m for D-LH_2, a result that implies the mutation is likely to be exerting a local effect on color determination. In our model, part of the Ile351 side-chain approaches the benzothiazole ring of D-LH_2 and this residue is located far from the Mg-ATP binding site, a position supported by our findings. Overall, the bioluminescence results suggest that the C-terminal residues of the β-hairpin motif play an important role in determining the color of light emission.

The R218A mutant emitted red light and the role of Arg218 in color determination has been studied previously (*31*). Our model predicts that the side-chain guanidinium group of Arg218 anchors the benzothiazole ring of D-LH_2 in the binding pocket through hydrogen-bonding interactions with the phenolate group. We believe that invariant Arg218 provides electrostatic and hydrogen-bonding interactions with the keto form of the emitter that are important for normal bioluminescence. The side-chain hydroxyl group of Ser347 and the main chain carbonyl group of Ala348 are hydrogen-bonded to Arg218 in our model and both S347A and A348V were red emitters, although the S347A emission is bimodal with maxima at 601 and 557 nm in a relative ratio of 2:1. Although approximately half of the mutants had broadened emission spectra as indicated by the bandwidth data (Table 1), only S347A showed more than one distinct maximum. It is possible, however, that all firefly bioluminescence spectra are bimodal with either the short or long wavelength emission dominating. Possibly, altered interactions of the Ser347 and Ala348 mutants with Arg218 modify the ability

of the Arg residue to maintain essential interactions for normal yellow-green bioluminescence. Viviani et al. (*39*, *41*) have reported several examples of mutations of Arg residues at equivalent positions in railroad worm luciferases that support our work. However, in *Pyrearinus termitilluminans*, an Arg to Ser mutation did not alter bioluminescence color (*39*). While this result may indicate that the role of invariant Arg218 is not of universal importance among all beetle luciferases, it is reasonable that the Arg to Ser change in one click beetle species is tolerated because a unique compensating interaction occurs.

By mutating the 15 predicted D-LH_2 binding site contact residues, red-shifted bioluminescence has been produced through changes spanning the primary sequence region Arg218−Ile351. With the exception of Arg218, all of these residues are found in β-sheet B of the N-terminal domain. Significantly, we have demonstrated that the region Thr343−Ile351 of a β-hairpin motif is important for the yellow-green bioluminescence of Luc. Notably, mutations of residues distant from the D-LH_2 binding site, for example, His433 to Tyr and Pro450 to Ser in *Luciola cruciata* (His431 and Ala450 in Luc), have been shown to produce markedly red-shifted bioluminescence (*42*). An approximately 50 nm red shift also was observed (*43*) in the emission spectrum of the H433Y *Hotaria parvula* mutant. These examples in true fireflies are contrary to the findings based on chimeric railroad worm luciferases that residues beyond position 344 are not determinants of bioluminescence color (*41*). Pro450 is a far removed C-terminal domain residue, and the ability of this mutation to influence bioluminescence color may be related to a change in its relative position caused by a substantial conformation change similar to that observed in Acs (*27*).

Comparison of Substrate Specificity Determinants in Luc, Acs, DhbE, PheA, and the NRPSs. The determination of the PheA crystal structure (*25*) allowed for the decoding of substrate specificity of the amino acid adenylation domains of NRPSs (*44*, *45*). Using sequence alignments, 10 residues that form the phenylalanine-binding pocket in PheA were compared to the corresponding residues in other NRPSs and classified by their variability. From the results of mutagenesis studies of the 10 residues in PheA, a structural basis for substrate recognition among the NRPSs was advanced (*44*). Of the 10 residues comprising the binding site determinants for substrates Phe and DHB, seven (bold in Figure 3) correspond to Luc residues Gly246, Phe247, Phe250, Gly315, Ser347, Ala348, and Lys529 in the putative D-LH_2 binding pocket. Luc residues Leu286, Ala313, and Gly339 that correspond to the other common substrate pocket residues in PheA and DhbE were not examined in this study.

The mutated Luc residues Arg218, His245, Thr251, Gly316, Gly341, Leu342, Thr343, and Ile351 (Figures 2 and 3) are not significant to substrate binding in both the PheA and DhbE structures. Among this group of Luc residues, however, we note that His245 is in a similar position to the corresponding His234 whose imidazole side-chain in DhbE coordinates the carboxyl group of DHB. Phe234 of PheA cannot make this electrostatic interaction that is apparently not critical because in PheA, like DhbE and Luc, the invariant Lys517 (Lys529 in Luc) coordinates the carboxylate substrate. The interpretations of photooxidation and mutagenesis studies (*28*−*30*, *38*) of His245 and Lys529 made with our model prior to the publication of the DhbE structure are substantiated.

In PheA and DhbE, Trp239 (Phe250 in Luc) and Tyr236 (Phe247 in Luc) form the bases of the binding sites for Phe and DHB, respectively. In Acs, the propyl group is bound in a shallow pocket in a generally similar position as Phe in the PheA structure. The considerably smaller alkyl group is only in contact with three Acs residues (Val310, Val386, and Trp414) that correspond to Luc residues Gly246, Gly315, and Gly341, respectively. The deeper Phe pocket of PheA is terminated by a residue that is three positions advanced in the sequence compared to DhbE. Since D-LH_2 is larger than Phe, the Luc substrate pocket should be even deeper than that of PheA. In fact, our kinetics results (Table 1) for the Phe250 mutants are not consistent with this residue restricting the base of the pocket. Instead, we believe that the results reported here and elsewhere (*31*) for the Arg218 mutants justify our suggestion that the side-chain group of Arg218, stringently conserved among the luciferases, forms the base of a deeper substrate binding site.

One of two invariant substrate specificity-determining residues in the NRPSs corresponds to Lys529 in Luc and is stringently conserved in the acyl adenylate-forming superfamily. The other, Asp235 in PheA, coordinates the α-amino group of Phe and would be expected to make the same interaction with any amino acid activated by the NRPSs. In DhbE, the corresponding residue is Asn235, whose side-chain makes bivalent hydrogen-bonds to the 2′- and 3′-OH groups of DHB (*26*). The analogous Luc residue Gly246 is positioned near the thiazoline ring of D-LH_2 in our model, and its replacement by Ala produced kinetic properties very similar to those of PplGR.

Luc residues Phe247, Gly315, and Ser347 correspond to three moderately variable residues within the NRPSs that might modulate adenylation activity and fine-tune the specificity of the corresponding domains (*44*). Interestingly, DhbE residue Val337 (Ser347 in Luc) is one of two key residues that provide discrimination between natural substrate DHB and salicylate (*26*). Among the luciferases, Ser is substituted by Cys at position 347 in the firefly *Photuris* and in the railroad worms. Apparently, a larger and weaker hydrogen-bonding side-chain can be accommodated. Removal of the hydroxyl group by the Ala substitution in Luc, however, resulted in a significantly elevated K_m for D-LH_2 and an unusual bimodal emission spectrum (Table 1). Gly315 and Phe247 are stringently conserved in the luciferases and, as discussed above, are important for productive D-LH_2 binding.

Luc residues Phe250 and Ala348, corresponding to two of the highly variable and substrate recognition-determining residues in the NRPSs (*44*), were mutated in this study. Ala348 is invariant among the luciferases and the A348V enzyme had greatly elevated K_m values for both substrates (Table 1). These results suggest a different role for this residue than that found in the NRPSs. In fact, our model predicts that Ala348 is hydrogen-bonded to the side-chain group of Arg218, a residue that does not have an equivalent role in the NRPSs. As discussed above, Phe250 does not seem to have substrate specificity-determining properties in the luciferases.

CONCLUDING REMARKS

The results discussed here present additional substantiation for the usefulness of our previously published working model of the Luc active site in providing a rational basis for mutagenesis studies. While focusing on the putative D-LH_2 binding site, we have provided additional information regarding the difficult problem of beetle bioluminescence color determination. Additionally, Gly341 was identified as a residue that may be critical for catalysis, providing the basis for future studies. Furthermore, we have provided a foundation for ongoing studies designed to produce luciferase enzymes with altered substrate specificity for synthetic D-LH_2 analogues.

ACKNOWLEDGMENT

We thank Marc Zimmer for performing molecular graphics experiments and Rachelle Magyar, Nate Portier, Justin Stroh, Neelum Khattak, and Evelyn Bamford for technical assistance.

REFERENCES

1. DeLuca, M. (1976) *Adv. Enzymol. 44*, 37−68.
2. Wood, K. V. (1995) *Photochem. Photobiol. 62*, 662−673.
3. Wilson, T., and Hastings, J. W. (1998) *Annu. Rev. Cell. Dev. Biol. 14*, 197−230.
4. White, E. H., Rapaport, E., Seliger, H. H., and Hopkins, T. A. (1971) *Bioorg. Chem. 1*, 92−122.
5. Contag, C. H., and Bachmann, M. H. (2002) *Annu. Rev. Biomed. Eng. 4*, 235−260.
6. Greer, L. F., III, and Szalay, A. A. (2002) *Luminescence 17*, 43−74.
7. Kricka, L. J. (1995) *Anal. Chem. 67*, 499R-502R.
8. Price, R. L., Squirrell, D. J., and Murphy, M. J. (1998) *J. Clin. Ligand Assay 21*, 349−357.
9. Kricka, L. J. (2000) *Methods Enzymol. 305*, 333−345.
10. Koo, J.-Y., Schmidt, S. P., and Schuster, G. B. (1978) *Proc. Natl. Acad. Sci. U.S.A.* 75, 30−33.
11. Seliger, H. H., and McElroy, W. D. (1960) *Arch. Biochem. Biophys. 88*, 136−141.
12. Wood, K. V., Lam, Y. A., Seliger, H. H., and McElroy, W. D. (1989) *Science 244*, 700−702.
13. Ye, L., Buck, L. M., Schaeffer, H. J., and Leach, F. R. (1997) *Biochim. Biophys. Acta 1339*, 39−52.
14. Viviani, V. R., Bechara, E. J. H., and Ohmiya, Y. (1999) *Biochemistry 38*, 8271−8279.
15. Viviani, V. R., Silva, A. C. R., Perez, G. L. O., Santelli, R. V., Bechara, E. J. H., and Reinach, F. C. (1999) *Photochem. Photobiol. 70*, 254−260.
16. Choi, Y. S., Lee, K. S., Bae, J. S., Lee, K. M., Kim, S. R., Kim, I., Lee, S. M., Sohn, H. D., and Jin, B. R. (2002) *Comp. Biochem. Physiol. Part B 132*, 661−670.
17. Lee, K. S., Park, H. J., Bae, J. S., Goo, T. W., Kim, I., Sohn, H. D., and Jin, B. R. (2001) *J. Biotechnol. 92*, 9−19.
18. Suzuki, H., Kawarabayasi, Y., Kondo, J., Abe, T., Nishikawa, K., Kimura, S., Hashimoto, T., and Yamamoto, T. (1990) *J. Biol. Chem. 265*, 8681−8685.
19. Babbitt, P. C., Kenyon, G. L., Martin, B. M., Charest, H., Sylvestre, M., Scholten, J. D., Chang, K.-H., Liang, P.-H., and Dunaway-Mariano, D. (1992) *Biochemistry 31*, 5594−5604.
20. Chang, K.-H., Xiang, H., and Dunaway-Mariano, D. (1997) *Biochemistry 36*, 15650−15659.
21. Fontes, R., Ortiz, B., De Diego, A., Sillero, A., and Günther Sillero, M. A. (1998) *FEBS Lett. 438*, 190−194.
22. Ortiz, B., Fernandez, V. M., Günther Sillero, M. A., and Sillero, A. (1995) *J. Photochem. Photobiol. B. Biol. 29*, 33−36.
23. Conti, E., Franks, N. P., and Brick, P. (1996) *Structure 4*, 287−298.
24. Franks, N. P., Jenkins, A., Conti, E., Lieb, W. R., and Brick, P. (1998) *Biophys. J. 75*, 2205−2211.
25. Conti, E., Stachelhaus, T., Marahiel, M. A., and Brick, P. (1997) *EMBO J. 16*, 4174−4183.
26. May, J. J., Kessler, N., Marahiel, M. A., and Stubbs, M. T. (2002) *Proc. Natl. Acad. Sci. U.S.A. 99*, 12120−12125.
27. Gulick, A. M., Starai, V. J., Horswill, A. R., Homick, K. M., and Escalante-Semerena, J. C. (2003) *Biochemistry 42*, 2866−2873.
28. Branchini, B. R., Magyar, R. A., Murtiashaw, M. H., Anderson, S. M., and Zimmer, M. (1998) *Biochemistry 37*, 15311−15319.
29. Branchini, B. R., Magyar, R. A., Murtiashaw, M. H., Anderson, S. M., Helgerson, L. C., and Zimmer, M. (1999) *Biochemistry 38*, 13223−13230.
30. Branchini, B. R., Murtiashaw, M. H., Magyar, R. A., and Anderson, S. M. (2000) *Biochemistry 39*, 5433−5440.
31. Branchini, B. R., Magyar, R. A., Murtiashaw, M. H., and Portier, N. C. (2001) *Biochemistry 40*, 2410−2418.
32. Ugarova, N. N., and Brovko, L. Y. (2001) *Russ. Chem. Bull., Int. Ed. 50*, 1752−1761.
33. Branchini, B. R., Murtiashaw, M. H., Magyar, R. A., Portier, N. C., Ruggiero, M. C., and Stroh, J. G. (2002) *J. Am. Chem. Soc. 124*, 2112−2113.
34. Thompson, J. F., Geoghegan, K. F., Lloyd, D. B., Lanzetti, A. J., Magyar, R. A., Anderson, S. M., and Branchini, B. R. (1997) *J. Biol. Chem. 272*, 18766−18771.
35. Morton, R. A., Hopkins, T. A., and Seliger, H. H. (1969) *Biochemistry 8*, 1598−1607.
36. Imai, K., and Goto, T. (1988) *Agric. Biol. Chem. 52*, 2803−2809.
37. Zoller, M. J., and Smith, M. (1983) *Methods Enzymol. 100*, 468−500.
38. Branchini, B. R., Magyar, R. A., Marcantonio, K. M., Newberry, K. J., Stroh, J. G., Hinz, L. K., and Murtiashaw, M. H. (1997) *J. Biol. Chem. 272*, 19359−19364.
39. Viviani, V. R., Uchida, A., Viviani, W., and Ohmiya, Y. (2002) *Photochem. Photobiol. 76*, 538−544.
40. Ramakrishnan, C., and Ramachandran, G. N. (1965) *Biophys. J. 5*, 909−933
41. Viviani, V. R., and Ohmiya, Y. (2000) *Photochem. Photobiol. 72*, 267−271.
42. Kajiyama, N., and Nakano, E. (1991) *Protein Eng. 4*, 691−693.
43. Ueda, H., Yamanouchi, H., Kitayama, A., Inoue, K, Hirano, T., Suzuki, E., Nagamune, T., and Ohmiya, Y. (1997) in *Bioluminescence and Chemiluminescence: Molecular Reporting with Photons* (Hastings, J. W., Kricka, L. J., and Stanley, P. E., Eds.) pp 7−15, John Wiley and Sons, Chichester.
44. Stachelhaus, T., Mootz, H. D., and Marahiel, M. A. (1999) *Chem. Biol. 6*, 493−505.
45. Challis, G. L., Ravel, J., and Townsend, C. A. (2000) *Chem. Biol. 7*, 211−224.
46. Kraulis, P. J. (1991) *J. Appl. Crystallogr. 24*, 945−950.

BI030099X